Available online at www.sciencedirect.com
ScienceDirect
Electrochimica Acta 52 (2007) 6569–6583
ELECTROCHIMICA Acta
www.elsevier.com/locate/electacta

Noise resistance and shot noise parameters on the study of IGC of aluminium alloys with different heat treatments

J.M. Sánchez-Amaya *, M. Bethencourt, L. González-Rovira, F.J. Botana

Departamento de Ciencia de los Materiales e Ingeniería Metalúrgica y Química Inorgánica, CASEM, Universidad de Cádiz, Avda. República Saharaui s/n, Apdo. 40, Puerto Real, 11510 Cádiz, Spain

Received 13 February 2007; received in revised form 13 April 2007; accepted 23 April 2007
Available online 29 April 2007

Abstract

In the present paper, the effect of heat treatment on the susceptibility to intergranular corrosion (IGC) of aluminium alloys is analysed. Samples of aluminium alloys AA2024 and AA7075 were first subjected to different heat treatments. Then the susceptibility of these samples to IGC was determined by means of normalized tests, based on the immersion of the samples in an aggressive medium and the subsequent evaluation of the attack, using metallographic analysis. In order to quantity the IGC suffered by the samples, both the degree and the depth of the attacks were measured. In addition, electrochemical noise (EN) signals were recorded during the normalized tests. This technique is especially interesting for the study of corrosion processes of systems with low impedance, such as those faced in this paper, since it does not modify the corrosion potential of the system. Three parameters were used to analyse the EN signals: noise resistance (R_n) and two shot noise parameters, the characteristic charge (q) and the characteristic frequency (f_n). Finally, the relationship between the results of the metallographic analysis and those obtained from the analysis of EN signals was established. Unfortunately, a poor correlation between the shot noise parameters and the degree of IGC was found, due to both the high localization and high activities of all systems.

Keywords: Aluminium alloys; Heat treatments; Intergranular corrosion; Electrochemical noise; Shot noise

1. Introduction

In general terms, when aluminium and aluminium alloys are not subjected to any hardening treatment, they are not hard enough to be employed for structural purposes. The mechanic strength of aluminium alloys can be increased by different mechanisms, such as plastic deformation (work hardening), alloying (solute hardening), precipitation hardening or reducing the grain size [1,2]. The aluminium alloys of highest mechanical strength, series 2xxx, 6xxx and 7xxx, can be hardened by precipitation. The main requirement of one alloy to be effectively treatable by precipitation hardening is that, in its phase diagram, the solubility of one or more alloying elements decreases notably with temperature [1]. The heat treatments associated with precipitation hardening processes usually involve three steps [3]:

- Solution heat treatment. This step involves a temperature increase in order to obtain a single phase, in which the alloying elements are dissolved.
- Quenching. The quenching consists of cooling the alloy, usually at a high rate, with the aim of obtaining a supersaturated solid solution of the alloying elements.
- Ageing. This is the controlled decomposition of the supersaturated solid solution, the objective of which is to form a fine dispersion of precipitates. This step can be carried out at different temperatures, and is called natural ageing if performed at room temperature, and artificial ageing or over-ageing, if performed at higher temperatures.

On the industrial scale, a particular heat treatment is required if the product made from the treated alloy has to satisfy a series of products requirements related to the intended application. These requirements are determined by the chemical and mechanical properties of the treated material [4]. Specifically in the aeronautical field, one of the requirements of aluminium alloys

* Corresponding author.
E-mail address: josemaria.sanchez@uca.es (J.M. Sánchez-Amaya).

0013-4686/$ – see front matter © 2007 Elsevier Ltd. All rights reserved.
doi:10.1016/j.electacta.2007.04.094

subjected to heat treatments is that they must present satisfactory behaviour against intergranular corrosion (IGC). In this context, the conditions in which the heat treatments are performed strongly influence the behaviour of aluminium alloys in resisting IGC.

The influence of the different steps of the heat treatment on the susceptibility to IGC of aluminium alloys has been studied in the literature. Thus, in [5] it is described that both solution and artificial ageing provoke changes in the mechanical properties and in the corrosion properties of the samples. These structural changes can be quite complex, since a great variety of processes can occur: particle dissolution, particle coarsening, precipitation, changes in dislocations distribution and density, and changes of composition and structure in grains and in grain boundaries [5]. According to [1], the optimum conditions to obtain samples with low susceptibility to IGC are: solution at high temperature, quenching at a high rate, and ageing at room temperature (natural ageing). Obviously, the specific conditions vary in function of the aluminium alloy and the shape of the samples.

The rate of quenching is a factor with great influence on the susceptibility to IGC in aluminium alloys. In this context, at low quenching rates, precipitation is produced at the grain boundaries, provoking an increase in susceptibility to IGC. In contrast, if the quenching rate is fast, precipitates cannot be formed at grain boundaries, and consequently, the behaviour against IGC is improved [6].

The effect of artificial ageing has also been analysed in the recent literature. The results reported in [6–8] demonstrate that this step has a strong influence on the susceptibility to IGC of aluminium alloy products. In general terms, when a sample is subjected to an over-ageing treatment, its properties will depend on the heat treatment that the sample initially had before this step. Thus, if the initial treatment is adequate, i.e., the sample has low susceptibility to IGC, artificial aging is expected to cause an increase in the susceptibility to IGC [9,10]. On the other hand, if the initial heat treatment is inappropriate, over-ageing can decrease the susceptibility of samples to IGC [9–11].

In the present paper, AA2024 and AA7075 samples have been subjected to different heat treatments, with the aim of modifying their susceptibility to IGC. Subsequently, a normalized test based on the immersion of the samples in a corrosive medium under controlled conditions was conducted to determine the susceptibility to IGC of these samples. After these tests, a metallographic analysis was carried out to quantify the IGC suffered by the samples. In addition, electrochemical noise has been measured during these normalized tests. This electrochemical technique has been widely used to study both the activity and the mechanism of different corrosive systems [12–21]. It has the advantage of not modifying the corrosion potential of the system studied. Therefore, electrochemical noise is especially interesting for measuring systems of low impedance, like those faced in the present paper. The objective of this paper is to correlate the results obtained with the metallographic evaluation and those obtained from the analysis of electrochemical noise.

2. Experimental

As described above, the effect of heat treatment on the degree of IGC suffered by samples of AA2024 and AA7075 has been analysed. The composition of these alloys is given in Tables 1 and 2. It can be emphasised that the objective of this paper is not to validate the heat treatment, but to correlate the degree of IGC shown by the various aluminium alloys samples, with the characteristics of the EN signals generated during the tests. In continuation, the heat treatments performed are detailed.

2.1. Heat treatments

In order to induce different degrees of IGC in the aluminium alloy samples, the heat treatments included in Fig. 1 were performed. In the T_A treatment, the steps recommended by the standard AMS H-6088B [4] were followed, consisting of a solution heat treatment between 488 and 499 °C, and a subsequent fast quenching (quenching time less than 10 s). In the T_B treatment, the quenching time was increased over that of T_A, while in the T_C treatment, the solution temperature was increased over that of T_A. In all cases, a natural ageing was carried out, consisting of keeping the samples at room temperature for at least 1 week. A treatment similar to T_A has recently been applied to samples of aluminium alloys of the series 6xxx [8], but the ageing of samples performed in [8] was artificial.

The samples of the aluminium alloy AA2024 studied in the present paper were those subjected to T3 (initial treatment of the samples), T_A and T_B. The treatment T_C provoked deformation in AA2024 samples, and consequently, these samples were not

Table 1
Composition of the aluminium alloy AA2024

Si	0.103
Fe	0.252
Cu	4.42
Mn	0.62
Mg	1.46
Zn	0.182
Ni	<0.002
Cr	0.012
Pb	<0.002
Sn	0.009
Ti	0.018
Ag	0.000
B	0.001
Be	0.000
Bi	<0.002
Ca	0.001
Cd	0.000
Na	0.000
Sr	0.000
Li	0.000
Zr	0.002
Co	<0.001
V	0.011
Ga	0.009
Al	92.893
P	0.002

Table 2
Composition of the aluminium alloy AA7075

Si	0.068
Fe	0.275
Cu	1.59
Mn	0.044
Mg	2.36
Zn	5.74
Ni	0.003
Cr	0.192
Pb	<0.002
Sn	0.002
Ti	0.019
Ag	0.002
B	0.002
Be	0.001
Bi	<0.002
Ca	0.000
Cd	0.000
Na	0.000
Sr	0.000
Li	0.000
Zr	0.001
Co	<0.001
V	0.007
Ga	0.009
Al	89.681
P	0.001

studied. The AA7075 samples studied were those subjected to T_A, T_B and T_C treatments.

2.2. Evaluation of the susceptibility to IGC

The standard ASTM G 110-92 has been employed to evaluate the susceptibility to IGC of aluminium alloy samples [22]. According to this procedure, samples must be immersed during 6 h in an aqueous solution of NaCl 5.7% and H_2O_2 0.3%. Some specific exposure conditions are also detailed in this procedure: the solution temperature should be $30 \pm 3\,^{\circ}C$; the minimum solution volume should be 5 mL/cm^2 of metal surface exposed; and the immersion time should not be less than 6 h. After these normalized tests, metallographic images of the corroded samples were studied to evaluate the intergranular attack.

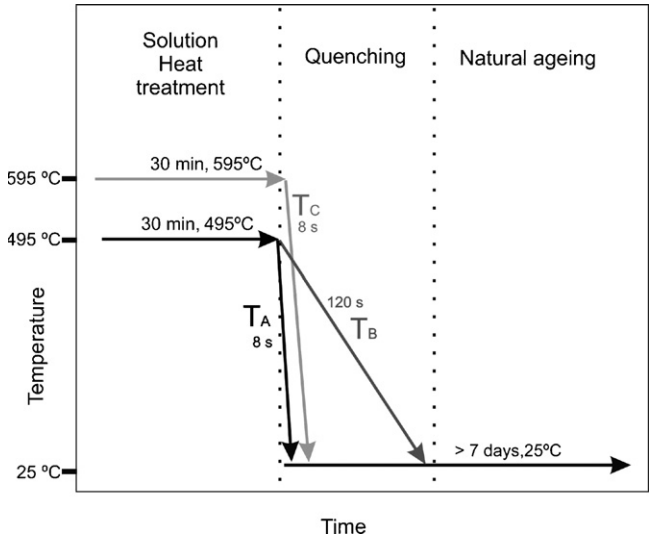

Fig. 1. Description of the heat treatments T_A, T_B and T_C.

The standard ASTM G 110-92 also recommends carrying out a surface cleaning procedure before immersing the samples in the NaCl and H_2O_2 solution. The first step of this cleaning procedure is an etching of the surface, in which samples are exposed in an acid solution (5 mL HF 40% and 50 mL HNO_3 69% per litre) for 1 min at 95 °C. After that, samples are rinsed with distilled water. Secondly, samples are exposed for 1 min in HNO_3 69% and rinsed again with distilled water.

During the immersion tests, EN signals of the systems were recorded. Therefore, the conditions recommended by the standard ASTM G 110-92 have been taken into account in the design of the electrochemical cell employed for measuring EN. This electrochemical cell will be described later.

The standard ASTM G 110-92 does not include any defined criterion for evaluating the IGC attack suffered by the samples during the tests. For this reason, an internal criterion has been elaborated with the object of estimating the extent of IGC. Both qualitative and quantitative analyses were carried out from the study of the metallographic images of the samples subjected to the normalized tests. Both the qualitative and the quantitative analyses are described in continuation:

- Qualitative analysis.

  The qualitative analysis comprises an evaluation of the attack morphology of the sample surface after the tests of susceptibility to IGC. For this purpose, five degrees of IGC were defined, in function of the number of grain layers affected by the attack. In these tests, in addition to the IGC attack, pits usually appear in the samples. Thus, samples that do not show IGC undergo only pitting corrosion. For this reason, a sixth degree of attack has been incorporated, which is employed to designate the samples that only undergo pitting corrosion. Therefore, the qualitative analysis of the AA2024 and AA7075 samples was carried out taking into account six degrees of attack, which range between pure pitting corrosion and extreme IGC, Table 3. In this table the code letters "P", "A", "B", "C", "D" and "E" are employed to designate these degrees.

  It should be noted that the same sample can present several zones with different degrees of attack. As a consequence, it is necessary to define parameters that describe the characteristics of the grade or degree of damage. Thus, two parameters have been proposed: the "Average Grade", G_A and the "Maximum Grade", G_M. The parameter G_A can be defined as the grade of attack most repeated over the sample surface, that is, the predominant grade. Meanwhile, the parameter G_M is the maximum grade of attack observed in the sample.
- Quantitative Analysis.

  The quantitative analysis is based on measurement of the depth of corroded zones. In this paper, two parameters have been defined to evaluate the depth of the attacks produced in the normalized IGC tests: the "Maximum Depth", D_M, and the "Average Depth", D_A. Since the most important characteristic

Table 3
Types of attack defined to evaluate the damage suffered by the aluminium alloy samples subjected to normalized IGC tests

Type of attack	Code	Definition
Pitting corrosion	P	After the test, the area exposed only shows pits. Signs of IGC are not observed
IGC. Degree A	A	In the affected zones, ramifications tracing the shape of grains can be distinguished, although whole grains are not revealed
IGC. Degree B	B	Some whole grains in the attacked zones can be seen in the metallographic images
IGC. Degree C	C	In the affected area, two layers of attacked grains can be appreciated
IGC. Degree D	D	Up to three layers of grains are defined in the metallographic images of the corroded zones
IGC. Degree E	E	Maximum sensitivity of samples to attack (extreme IGC). In the corroded zones, more than three layers of grains are defined

of each sample is the zones suffering most attack, the average depth has been estimated from the five deepest focuses of attack found in the samples.

As will be shown later, in AA7075 samples it is of interest to estimate the horizontal extent of the attack, that is, the width or diameter of the affected zones. Two parameters have been used to quantify the horizontal attack in these samples: the Maximum Width, W_M, and the Average Width, W_A.

2.3. Measurements of electrochemical noise

It should be emphasised that some corrosion mechanisms, especially localized processes such as pitting corrosion or IGC, show a significant stochastic component, since it is not possible to predict accurately either the moment or the place in which these localized attacks are going to happen in the samples. As a consequence, the experiments in which localized corrosion processes are developing are relatively irreproducible [13]. For this reason, in the present paper, the EN was recorded during the normalized tests, and therefore the EN was produced by the same samples which were evaluated with the metallographic analysis. This procedure enables us to correlate the characteristics of the EN signals with the degree of IGC observed in the metallographic analysis. The experimental equipments employed specifically enabled the recording of EN signals during the normalized immersion tests.

In order to measure the EN signals, a modification of the "Parc" single cell was employed, which allows two working electrodes to be exposed to the standard solution. A schematic illustration of the cell developed has been included in Fig. 2. An anticorrosive adhesive tape with a central aperture of 0.79 cm^2 was applied to each working electrode. This adhesive tape has two functions: first, it reduces the crevice corrosion, and second, it delimitates the area of the working electrode exposed to the solution. To comply with the normalized tests for the detection of susceptibility to IGC [22], a minimum of 5 mL of solution per cm^2 of metal surface exposed is required. This requirement has been fully satisfied, since in each test 1.58 cm^2 of surface was exposed in 300 mL of solution. It should be clarified that the

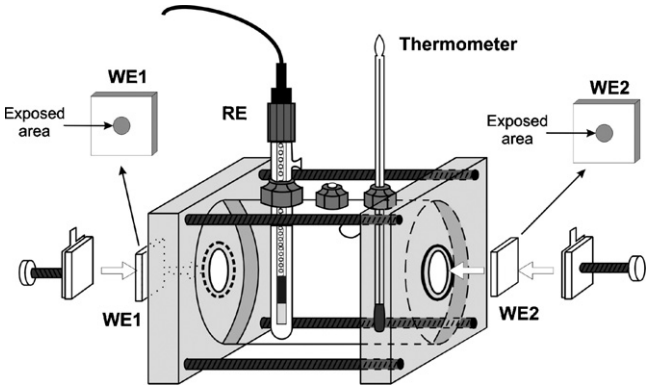

Fig. 2. Schematic illustration of the cell employed to conduct the IGC tests, which allows the measurements of EN.

normalized tests do not specify that it is necessary to delimitate the exposure area of the samples. However, it has been demonstrated in the literature that some control of the area exposed is essential in electrochemical noise tests [13,16,23–28].

The electrochemical noise current and voltage signals were recorded simultaneously using a potentiostat 1287 of Solartron Instruments (1287SI), connected to a computer by means of an IEEE-488 GPIB ("General Purpose Interface Bus") of National Instruments. The software "CorrWare" of "Scribner" was used to control the electrochemical noise measurements. Aliasing is a typical problem related with analogical to digital conversion, which appears when a sampling rate is not high enough to measure the signals fluctuations. The existence of aliasing generates artefacts in the signals and can be detected when a plateau at the high frequency region of PSD is observed. In order to avoid aliasing, a digital filter of 2 Hz was activated during the EN measurements in this work. This anti-aliasing filter carries out a fast average in the time domain, allowing an actual data acquisition rate of 2.16 Hz. According to the literature [29], this is an effective method to avoid aliasing in EN measurements.

Following the standard ASTM G-110 recommendations for IGC tests, the duration of the tests was exactly 6 h. Since the authors wanted to obtain one record per hour of exposure and calculate the PSD of the records, they have to contain 2^n data. Thus, one record of 4096 points at 2.16 Hz was stored during the last 32 min of each 6 h.

2.4. Parameters of analysis of electrochemical noise

Three parameters have been employed to analyse the EN signals generated during the normalized tests: the noise resistance (R_n), the characteristic charge (q) and the characteristic frequency (f_n).

The parameter R_n was proposed for the first time by Eden [30], and can be estimated by dividing the standard deviation of potential noise by the standard deviation of the current noise signal [13,31]:

$$R_n = \frac{\sigma_E}{\sigma_I} \quad (1)$$

R_n is inversely proportional to the corrosion rate when both working electrodes have the same activity and the corrosion pro-

cess is uniform under activation control [13,14,18]. However, even if the corrosion process is not strictly uniform, high R_n values are usually obtained when the system shows low activity, while low R_n values can be related to a high activity [13,18].

The characteristic charge (q) and the characteristic frequency (f_n) are parameters derived from the shot noise theory, and can be estimated by means of the following equations [13,16,24,18,32]:

$$q = \frac{\sqrt{\mathrm{PSD}_E\,\mathrm{PSD}_I}}{B} \quad (2)$$

$$f_n = \frac{B^2}{A\,\mathrm{PSD}_E} \quad (3)$$

where PSD_E and PSD_I are the PSD values of the potential noise and current noise measured at low frequency, respectively. B is the Stern–Geary coefficient and A is the exposed area of the working electrodes. In the present paper, the MEM method with order 50 was used to estimate PSD_E and PSD_I; the area exposed was 0.79 cm^2; and the value of the Stern–Geary coefficient was considered to be 0.026 V.

According to the literature [13,16,18,25,32–36], shot noise parameters, q and f_n, can be related to the predominant corrosion mechanisms of the systems studied. Thus, q is associated with the mass of metal lost in the corrosive events, while f_n informs us about the rate at which these events are happening [18,32,33]. Accordingly, a system in which an intense uniform corrosion is produced can lead to high values of q and f_n. On the contrary, localized corrosion processes like pitting corrosion and IGC usually present a small number of events, leading to high values of q and low values of f_n. Finally, the charge of passive systems is typically low while the frequency depends on the processes that take place in the passive layer [32–34]. For example, in [34] it is observed that a passive system presents low charge and high frequency.

3. Results and discussion

In order to promote different degrees of IGC in aluminium alloys, different heat treatments were applied to samples of AA2024 and AA7075. As commented before, two steps of the heat treatment have been modified: the solution temperature and the quenching time. These treatments provoke different degrees of susceptibility to IGC in the samples. The main aim of this work is to correlate the metallographic observations of samples subjected to IGC tests with the characteristics of the electrochemical noise signals measured during these tests.

3.1. Metallographic evaluation

Metallographic images of AA2024 samples with T_A, T3 and T_B heat treatments after the IGC tests are included in Figs. 3–5, respectively. In Fig. 3, it can be observed that samples with T_A treatment only showed pits, not presenting IGC attacks. In metallographic images of AA2024-T3 taken at high magnifications, Fig. 4, both pitting and IGC can be appreciated. In this case, the IGC is defined by only one layer of grains, so the degree of IGC is rated as low. In Fig. 5 it can

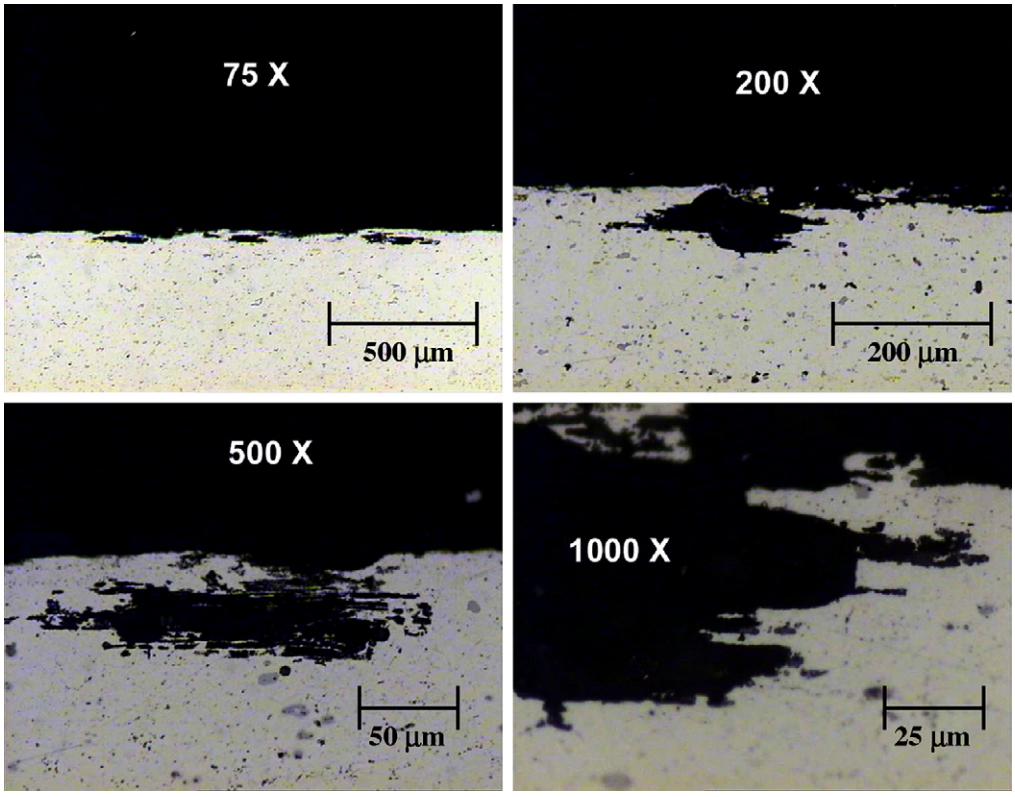

Fig. 3. Metallographic images of AA2024 samples with T_A heat treatment, after 6 h of exposure in NaCl 5.7% and H_2O_2 0.3% solution at 30 °C.

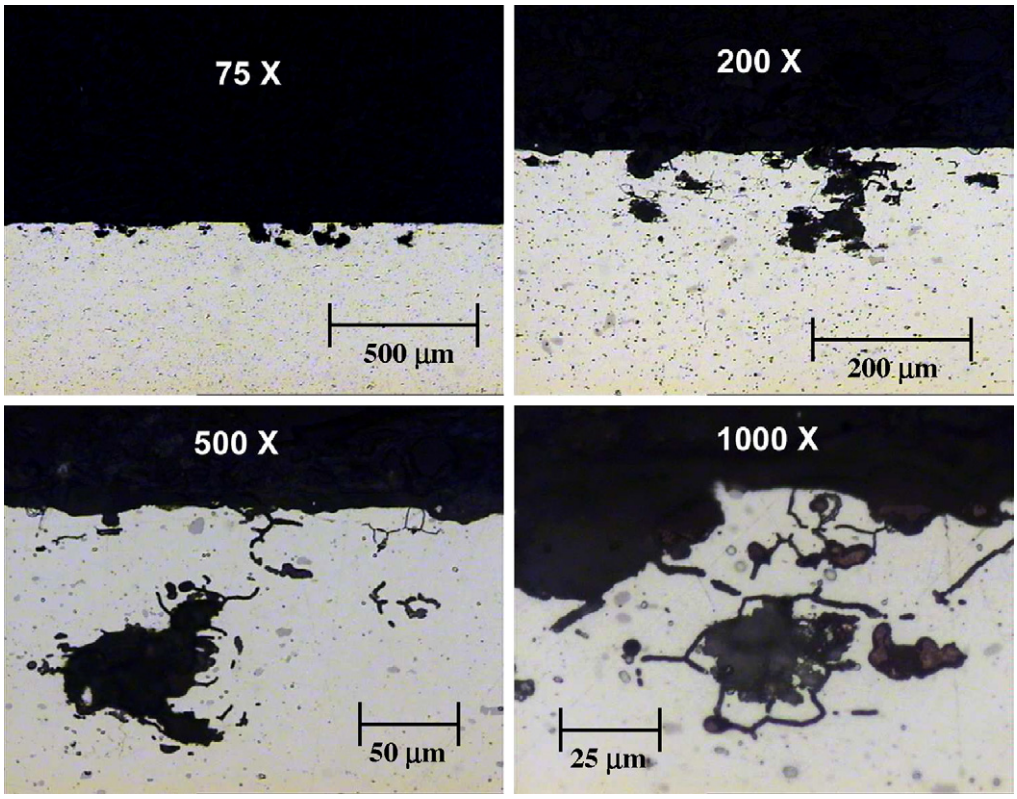

Fig. 4. Metallographic images of AA2024 samples with T3 heat treatment, after 6 h of exposure in NaCl 5.7% and H_2O_2 0.3% solution at 30 °C.

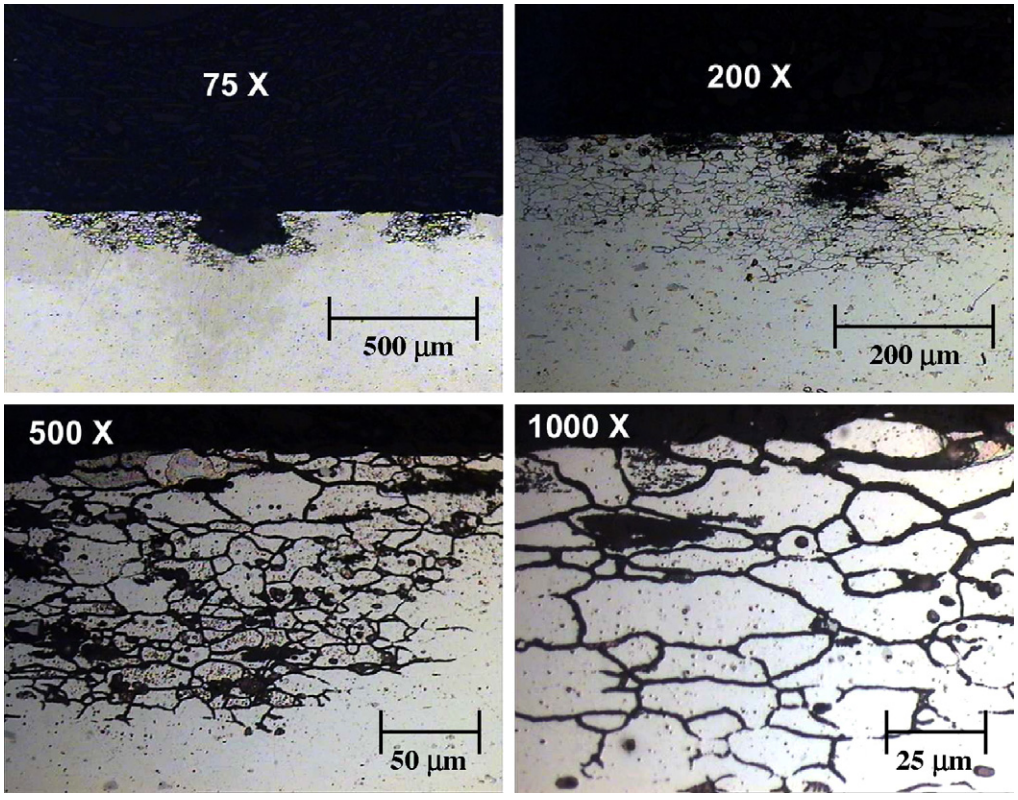

Fig. 5. Metallographic images of AA2024 samples with T_B heat treatment, after 6 h of exposure in NaCl 5.7% and H_2O_2 0.3% solution at 30 °C.

Table 4
Evaluation of AA2024 samples after the normalized IGC tests in function of the heat treatments

AA2024	Qualitative analysis (codes defined in Table 3)		Quantitative analysis (depths of attacks in μm)	
	G_A (average grade)	G_M (maximum grade)	D_A (average depth)	D_M (maximum depth)
T_A	P	P	81	101
T3	A	B	133	163
T_B	E	E	203	244

be seen that AA2024-T_B samples undergo extreme IGC, since the IGC extends down through several layers of grains.

From the metallographic analysis of the AA2024 corroded samples, Table 4 has been constructed; this includes the values of the parameters G_A, G_M, D_A and D_M, defined in Section 2.2 of this paper. These parameters allow one to quantify the differences that the heat treatments provoke in the behaviour against IGC of AA2024 samples. From this table it can be clearly verified that the quenching time has a considerable influence on both the type and the depth of the attacks. Concerning the corrosion type, the results given in Table 4 indicate that if the quenching time is long, the samples suffer mainly IGC rather than pitting corrosion. Thus, in AA2024-T_A samples, both G_A and G_M are "P", which indicate that only pits are observed; in AA2024-T3 samples, G_A and G_M are "A" and "B", respectively; while in AA2024-T_B, both G_A and G_M are "E", that is, the maximum degree of IGC. The parameters D_M and D_A from this Table 4 permit quantification of the attack depths in these samples. It can be observed that for each heat treatment, the D_M value is approximately 20% higher than the D_A value. From the analysis of D_M and D_A values, it can be seen that the attack depths are notably different when AA2024-T_A and AA2024-T_B are compared. Both D_M and D_A values for AA2024-T_B samples are more than double those for AA2024-T_A samples. According to these data, in AA2024 samples, the longer the quenching time of the heat treatment, the deeper the corrosion attack produced in the IGC test. This behaviour agrees with the results reported in the literature [6], where aluminium alloy samples previously subjected to heat treatments with high quenching times showed high susceptibility to IGC. Thus, both the degree and the depth of attacks increase when the quenching time is longer [6].

In continuation, results of the analysis of AA7075 samples after the normalized IGC tests are described. These samples were previously subjected to three different heat treatments, which have been designated in Fig. 1 as T_A, T_B and T_C. The metallographic images obtained after the tests are presented in Figs. 6–8.

Figs. 6 and 7 show metallographic images obtained after IGC tests of AA7075 samples with T_A and T_B heat treatments, respectively. If these figures are compared with Figs. 3 and 5, it can be seen that the attack morphology in AA7075 samples is different from that produced in AA2024 samples. The attacks on AA2024 are produced from different starting points, usually from pits, and spread through the zones surrounding these focal points. In contrast, the attack on the AA7075 samples is parallel to the surface, with morphology similar to that observed in aluminium alloy samples subjected to exfoliation tests [37]. Therefore, in order to evaluate the damage suffered by the AA7075 samples, it is necessary to introduce new parameters that take into account the horizontal extension of the attack, parallel to the surface exposed to the solution. Thus, two extra parameters have been estimated, the maximum width, W_M, and the average width, W_A.

When the metallographic images of AA7075-T_A samples, Fig. 6, are compared with images of AA7075-T_B, Fig. 7, it can be observed that the attack depth and morphology are quite similar. This similarity can be confirmed by analysing Table 5, which contains the results obtained when AA7075 samples were evaluated according to the criteria defined in Section 2.2. However, some differences were found between AA7075-T_A and AA7075-T_B samples. Thus, the attacks on AA7075-T_A samples usually initiate in pits, while in AA7075-T_B samples attacks do not start in pits and show a wider horizontal spread. This means that the attacks on AA7075-T_B are wider and shallower than in AA7075-T_A. Note, however, that these minor differences contrast with the results obtained with AA2024 samples, where major differences in both the depth and degree of the IGC were observed between T_A and T_B.

According to the criteria defined in Table 3, the maximum degree of IGC (D_M) reached by both AA7075-T_A and AA7075-T_B samples is "A", since the attack never affects whole grains. Meanwhile, G_M in AA7075-T_C samples is "P", reflecting that these samples did not undergo any kind of IGC. On the other hand, the G_A parameter coincides with G_M in AA7075-T_B and AA7075-T_C systems, which implies that the predominant attack is the same as the maximum attack observed: "P" in AA7075-T_C and "A" in AA7075-T_B. However, G_A and G_M of the system AA7075-T_A are different ("P" and "A", respectively). This means that the predominant attack is caused by pitting corrosion, although some focuses of IGC have been detected.

Results given in Table 5 also indicate that there are differences between AA7075-T_A and AA7075-T_B samples in both the depths and widths of attacks. These differences have been quantified by the D_A and D_M parameters. Thus, D_A in AA7075-T_A system was 128 μm, while 109 μm in AA7075-T_B. Similarly, D_M in AA7075-T_A was 155 μm, and 143 μm in AA7075-T_B. Therefore, samples with T_A treatment are attacked to greater depths than samples with T_B. However, it can be appreciated that the values of both W_M and W_A parameters are much higher in AA7075-T_B than in AA7075-T_A samples. Thus, W_A in samples with T_B treatment (606 μm) is almost double the value measured in those with T_A (361 μm). Similarly, the value of W_M is also higher in AA7075-T_B (775 μm) than in AA7075-T_A (541 μm). To sum up, AA7075-T_A samples showed deeper attacks but with less width than AA7075-T_B samples. These data demonstrate that AA7075 samples with T_A treatment are more susceptible to

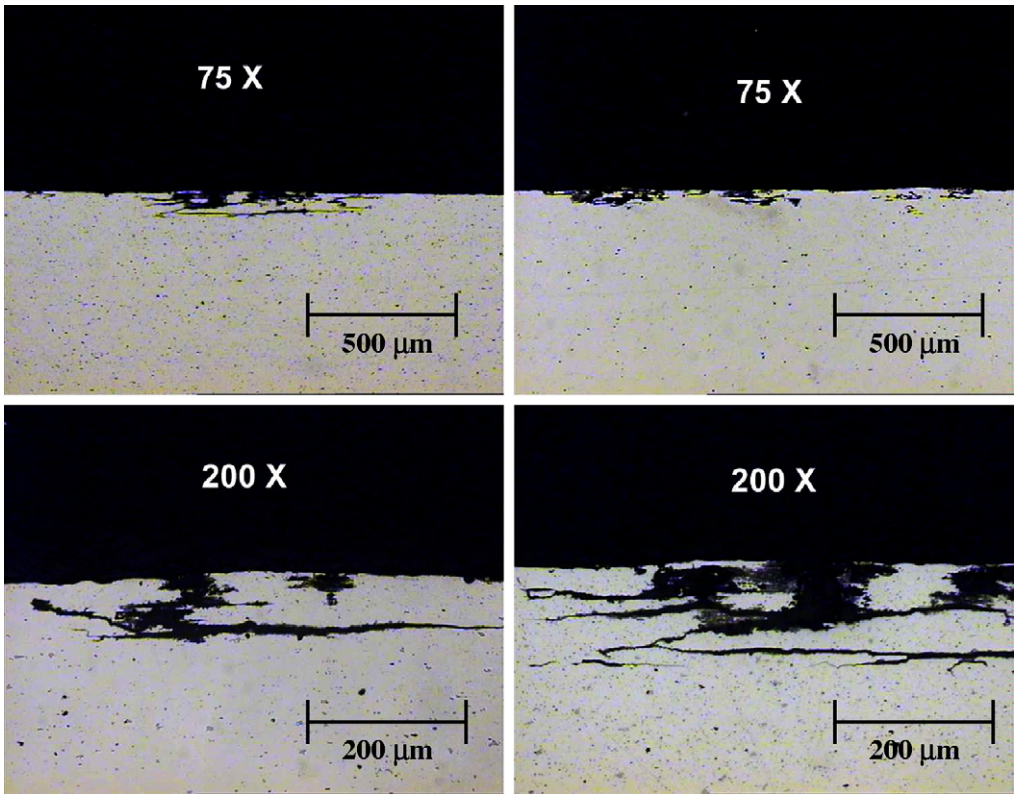

Fig. 6. Metallographic images of AA7075 samples with T_A heat treatment, after 6 h of exposure in NaCl 5.7% and H_2O_2 0.3% solution at 30 °C.

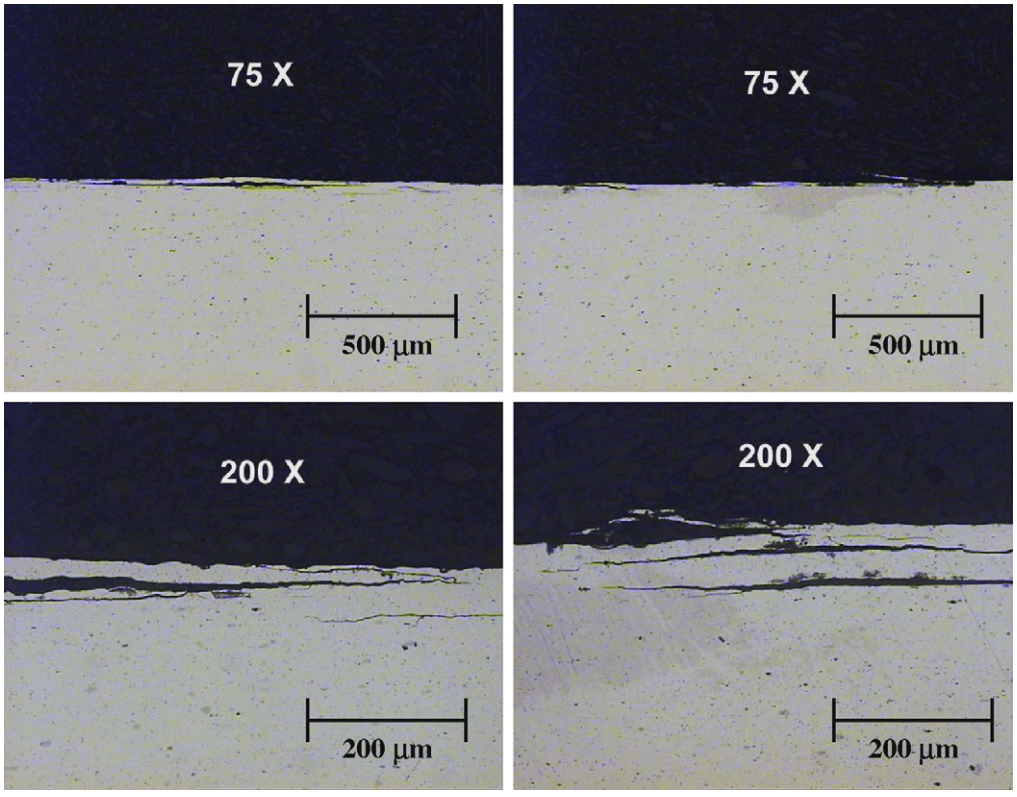

Fig. 7. Metallographic images of AA7075 samples with T_B heat treatment, after 6 h of exposure in NaCl 5.7% and H_2O_2 0.3% solution at 30 °C.

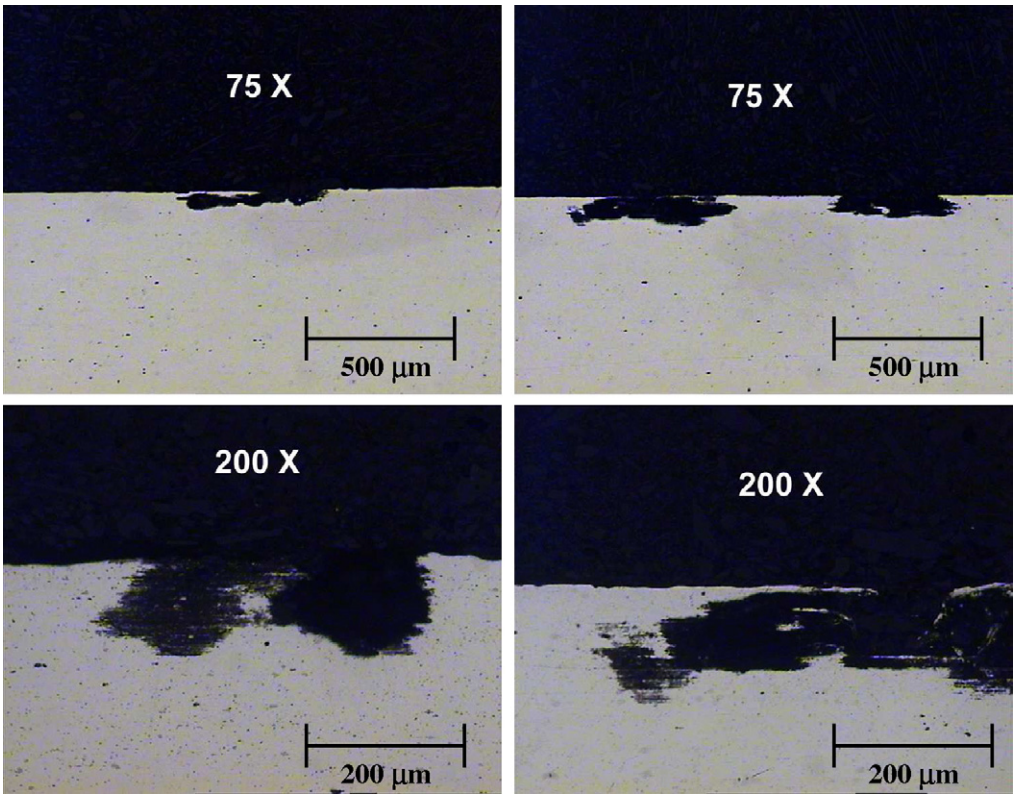

Fig. 8. Metallographic images of AA7075 samples with T_C heat treatment, after 6 h of exposure in NaCl 5.7% and H_2O_2 0.3% solution at 30 °C.

pitting corrosion than samples with T_B treatment, while samples with T_B are more susceptible to IGC parallel to the surface.

The metallographic images of AA7075-T_C samples after the IGC tests, Fig. 8, show that the surface exposed presents relatively few attacked zones, and almost the whole surface remains unaffected. In this figure it can be appreciated that the attack type is exclusively pitting corrosion, and no signs of IGC are observed. Concerning the morphology of these pits, it has been seen that they are not very deep, although some of them are relatively wide. The data included in Table 5 confirm that AA7075-T_C samples only showed pitting corrosion. Both the depth ($D_A = 111$ μm, $D_M = 158$ μm) and the width ($W_A = 532$ μm, $W_M = 199$ μm) of these pits have characteristics similar to those observed in AA7075 samples with T_A and T_B treatments. It can be emphasised that the number of pits found in AA7075-T_C samples was very low. However, this finding has not been reflected in the parameter values included in Table 5, since the average only quantifies the five deepest pits, not being evaluated either the amount or the density of pits in the surface exposed. Consequently, it can be concluded that T_C is the heat treatment that causes the least susceptibility to IGC in samples of AA7075.

In order to understand the different attack morphology seen in AA2024 and AA7075 samples subjected to the IGC tests, these samples were subsequently exposed to Keller's reagent, which reveals the grain microstructure of these alloys. The metallographic images obtained are included in Figs. 9 and 10. Fig. 9 shows that alloy AA2024 has equiaxial grains, characteristic that explains the form of the attack observed (Figs. 3–5). On the other hand, in Fig. 10 it can be observed that AA7075 has elongated grains, of much higher size than the grains of AA2024. The microstructure of the alloy AA7075 explains the special morphology of the intergranular attack seen in these samples. Therefore, it can be concluded that in both alloys, the morphology of the intergranular attack is determined by the grains shape.

When the results of the three heat treatments performed in AA7075 samples are compared, the order of susceptibility to IGC can be defined: AA7075-T_B > AA7075-T_A > AA7075-T_C. In comparison, the order of susceptibility to IGC in

Table 5
Evaluation of AA7075 samples after the normalized IGC tests in function of the heat treatments

AA7075	Qualitative analysis (codes defined in Table 3)		Quantitative analysis (depths and widths of attacks in μm)			
	G_A (average grade)	G_M (maximum grade)	D_A (average depth)	D_M (maximum depth)	W_A (average width)	W_M (maximum width)
T_A	P	A	128	155	361	541
T_B	A	A	109	143	606	775
T_C	P	P	111	158	532	799

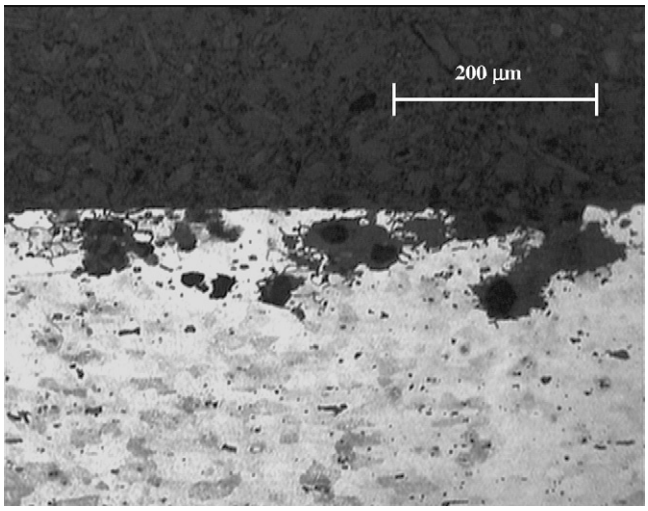

Fig. 9. Metallographic image of an AA2024-T3 sample, after 6 h of exposure in NaCl 5.7% and H_2O_2 0.3% solution at 30 °C and subsequently revealed with Keller's reagent.

AA2024 samples was the following: AA2024-T_B > AA2024-T3 > AA2024-T_A. Although there are some differences, it can be appreciated that the heat treatment that leads to the highest degree of IGC in both alloys is T_B, that is, the treatment with the slowest quenching step (longest quenching time).

3.2. Analysis of electrochemical noise

As commented before, electrochemical noise signals were recorded during the IGC tests. Some typical potential and current records, and their PSDs, have been included in Figs. 11–14. In Figs. 11 and 12, no pattern of individual events can be clearly observed, due to the high activities of the systems. Fig. 15 presents the R_n values of AA2024 samples with different heat treatments in function of the exposure time. It should be noted that, in general terms, all systems studied here lead to very low

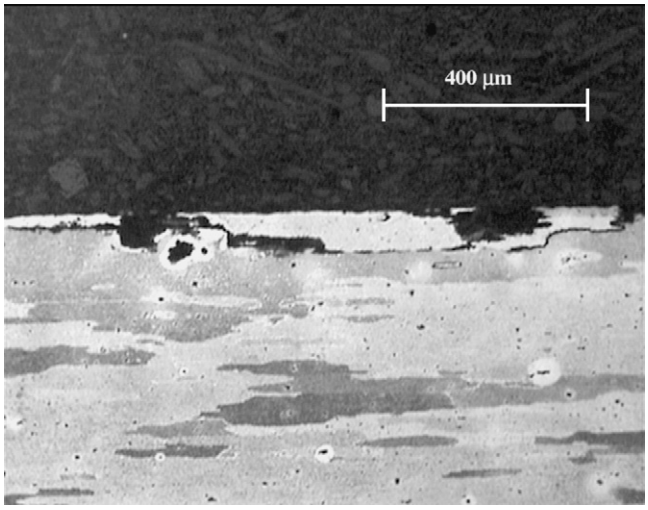

Fig. 10. Metallographic image of an AA7075-T_A sample, after 6 h of exposure in NaCl 5.7% and H_2O_2 0.3% solution at 30 °C and subsequently revealed with Keller's reagent.

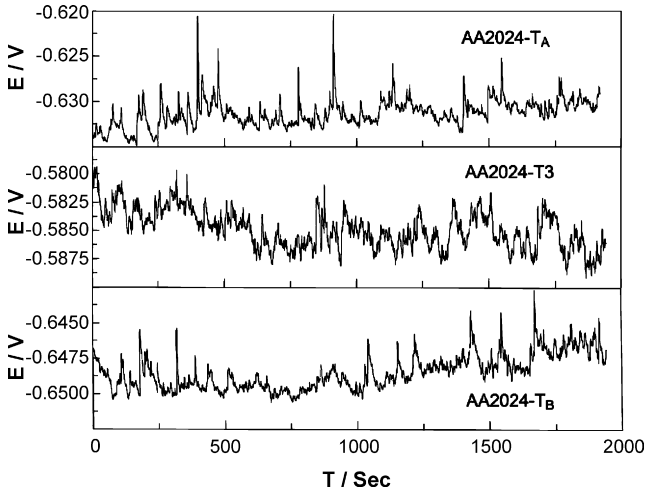

Fig. 11. Typical potential noise records obtained during the normalized IGC tests. Records taken at the first hour of exposition in samples of AA2024-T_A, AA2024-T3 and AA2024-T_B.

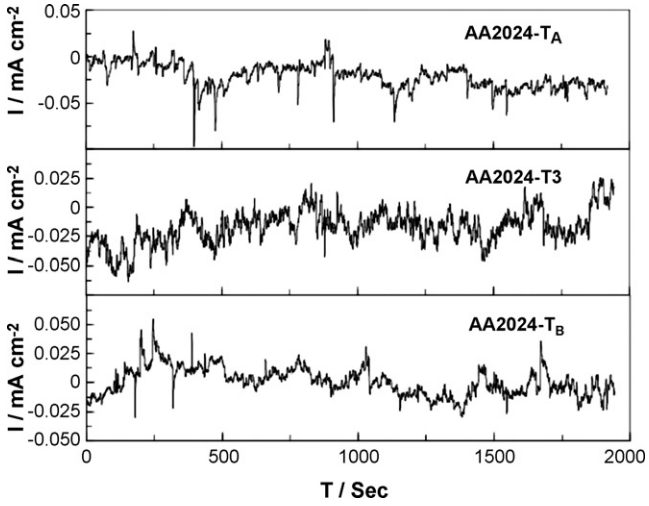

Fig. 12. Typical current noise records obtained during the normalized IGC tests. Records taken at the first hour of exposition in samples of AA2024-T_A, AA2024-T3 and AA2024-T_B.

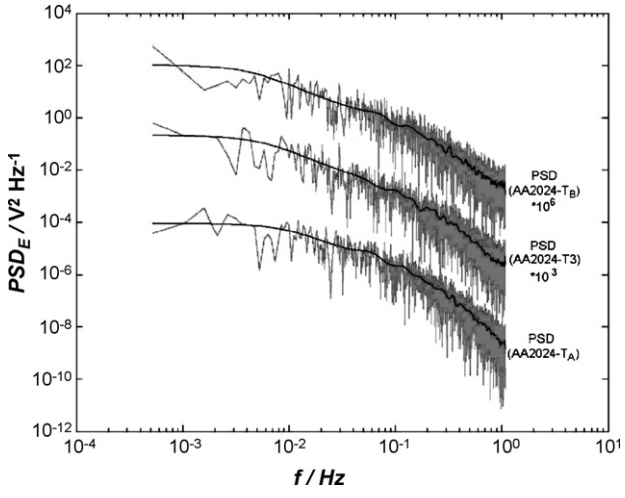

Fig. 13. PSDs estimated with FFT (in grey) and MEM of order 50 (in black) of the potential records included in Fig. 11.

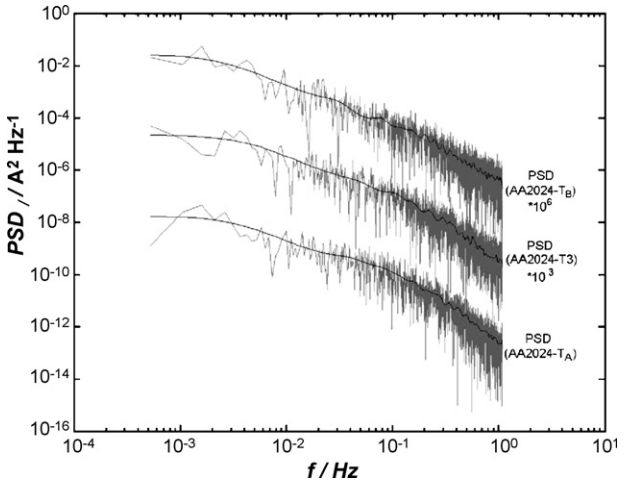

Fig. 14. PSDs estimated with FFT (in grey) and MEM of order 50 (in black) of the current records included in Fig. 12.

R_n values [18]. This is understandable considering the high reactivity of the corrosive medium employed. In Fig. 15, it can be observed that R_n values for AA2024-T_B are lower than those obtained for T3, and values for T3 are lower than those for T_A. Therefore, in the AA2024 samples, R_n values are slightly higher when susceptibility to IGC is lower. These results agree with those obtained from metallographic analysis, since, as commented before, both the attack degree and depth were high when the quenching time was long.

In Fig. 15, it can be also appreciated that R_n values generally increase with the exposure time for the three heat treatments studied. Since the parameter R_n is inversely proportional to the corrosion activity [13], it can be stated that the corrosion activity of the three systems studied decreases with the immersion time. However, it can be observed that all heat treatments lead to a minimum in the R_n values, this minimum being different for each system. Thus, in the heat treatment T_A, the minimum is reached at the third hour of exposure; in T3, at the second hour; and in T_B the minimum is observed at the first hour. The minimum R_n corresponds to a maximum in the corrosion activity. This maximum is always followed by a decrease in activity, which is thought to be due to the consumption of H_2O_2 from the

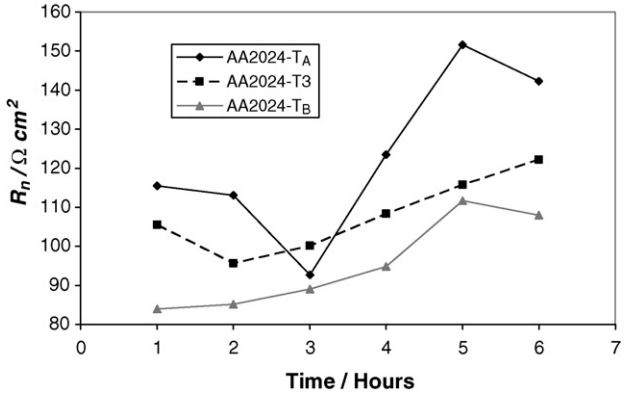

Fig. 15. R_n values of AA2024 samples in NaCl 5.7% and H_2O_2 0.3% solutions at 30 °C, in function of the heat treatment and the immersion time.

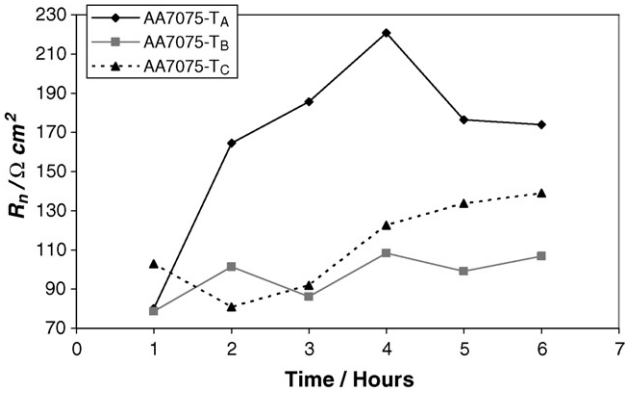

Fig. 16. R_n values of AA7075 samples in NaCl 5.7% and H_2O_2 0.3% solutions at 30 °C, in function of the heat treatment and the immersion time.

corrosive medium. The minimum R_n value for each heat treatment can be explained by considering the different reactivity of the metal samples. Thus, the most reactive AA2024 samples, those subjected to T_B treatment, are believed to consume the H_2O_2 from the solution very quickly. As a consequence, the minimum R_n appears at the first hour of the IGC test. Secondly, the samples of AA2024-T3 have an intermediate reactivity, the H_2O_2 of the solution being consumed at the second hour of exposure. Finally, the least reactive samples, AA2024-T_A, do not consume the H_2O_2 until the third hour, the minimum R_n being reached at this time. The minimum R_n values of each system were observed in at least three repeated tests, discarding the possibility that they are due to intrinsic experimental scattering. However, the assumption that the H_2O_2 depletion is the responsible of the minimum R_n value must be confirmed in future studies. In addition, the actual relationship between the H_2O_2 concentration and the R_n values, and the influence of the exposure time on the depth and grade of IGC, need to be analysed in further research.

Fig. 16 presents the evolution with exposure time of the R_n values of AA7075 samples with different heat treatments. These R_n values were obtained during the normalized IGC tests. In this figure, it can be seen that the order of the R_n values in the first hour of exposure coincides with the order of susceptibility to IGC of AA7075 samples stated above. Thus, in this first hour, the lowest R_n value was observed in the most active system, AA7075-T_B, while the highest value was obtained in the least active system, AA7075-T_C. A good correlation between the R_n values and the metallographic analysis (Table 5) was observed in AA7075-T_B samples, since for most exposure times, the lowest R_n values were obtained in this system. However, when systems AA7075-T_A and AA7075-T_C are compared, it can be seen that, after the second hour of exposure, the R_n values follow a trend different from that observed in the metallographic analysis. The difference between the two techniques is especially pronounced in the AA7075-T_A system, where particularly high R_n values were measured. As in Fig. 15, it can be observed in Fig. 16 that different heat treatments on AA7075 samples lead to different minimum R_n values. Thus, for the systems AA7075-T_A and AA7075-T_B, the minimum is reached at the first hour, while for AA7075-T_C, the minimum is observed at the second hour.

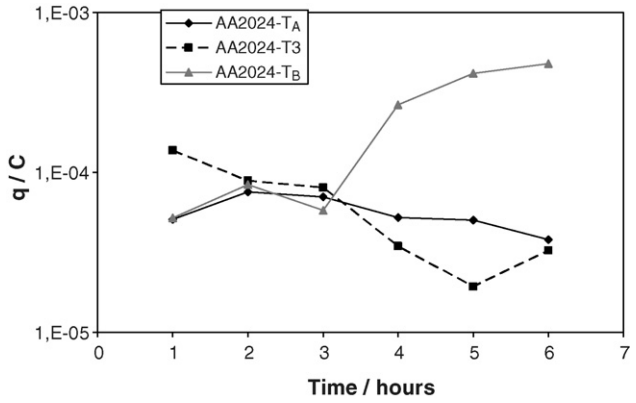

Fig. 17. q values of AA2024 samples in NaCl 5.7% and H_2O_2 0.3% solutions at 30 °C, in function of the heat treatment and the immersion time.

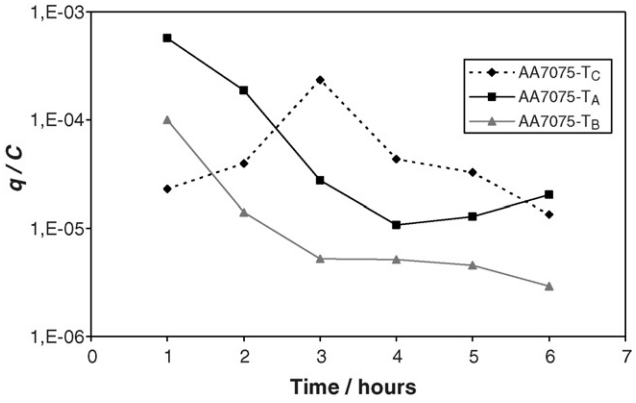

Fig. 19. q values of AA7075 samples in NaCl 5.7% and H_2O_2 0.3% solutions at 30 °C, in function of the heat treatment and the immersion time.

Although it has not been demonstrated, it is thought that the minimum values correspond to the time at which the H_2O_2 concentration is mostly consumed. Thus, the most passive system, AA7075-T_C, reacts more slowly with the H_2O_2 than the systems AA7075-T_A and AA7075-T_B. As a consequence, in AA7075-T_C the minimum R_n is observed later.

When R_n values obtained in AA2024 and AA7075 samples are compared, Figs. 15 and 16, it can be seen that these values have the same order of magnitude, all of them falling in the range from 80 to 150 Ω cm^2. Only the samples of AA7075-T_A showed higher values of this parameter.

Figs. 17 and 18 present the values of q and f_n corresponding to EN records obtained in AA2024 samples. Unfortunately, when q and f_n values of AA2024-T_A, AA2024-T3 and AA2024-T_B samples are compared, little information can be obtained about the corrosive processes of these systems, since few differences between shot noise values can be observed. However, it can be noted in Figs. 17 and 18 that, in the system AA2024-T_B after the third hour of exposure, the q value increases and the f_n value decreases. This indicates that in this system the number of events decreases with the exposure time, while the charge of these events increases. In contrast, EN signals obtained with T3 and T_B treatments show the reverse tendency. Thus, after the third hour of test, q values slightly decrease and f_n values smoothly increase with the exposure time.

The values of the shot noise parameters, q and f_n, obtained from the EN signals of AA7075 samples subjected to IGC tests, have been plotted in Figs. 19 and 20, respectively. In both figures, it can be appreciated that both q and f_n values are relatively similar for the three heat treatments applied. In addition, the values obtained in AA7075-T_A and in AA7075-T_B samples follow a similar trend, reflecting that both heat treatments lead to samples with analogous susceptibility to IGC. It should be recalled that in both samples, the IGC attack was parallel to the surface exposed.

In Fig. 19, it can be seen that after the third hour of exposure, q values show the following order: AA7075-T_B < AA7075-T_A < AA7075-T_C. It can be reminded from the metallographic analysis that the order of susceptibility to IGC in these samples was: AA7075-T_C < AA7075-T_A < AA7075-T_B. Thus, in tests with AA7075 samples, q values followed the reverse order compared with the susceptibility to IGC. Similarly, in Fig. 20 it can be seen that f_n values after the third hour of test generally follow the same order as the susceptibility to IGC. Therefore, it can be stated that the susceptibility to IGC in AA7075 samples is inversely related to q, and directly related to f_n values. Thus, the higher the susceptibility to IGC, the lower the q values, and the higher the f_n values. According to this conclusion, systems based on AA7075 samples that show high susceptibility to IGC have corrosion events with low charge and high frequency of appearance. However, the differences between the q and f_n values of the three heat treatments are very small, since the

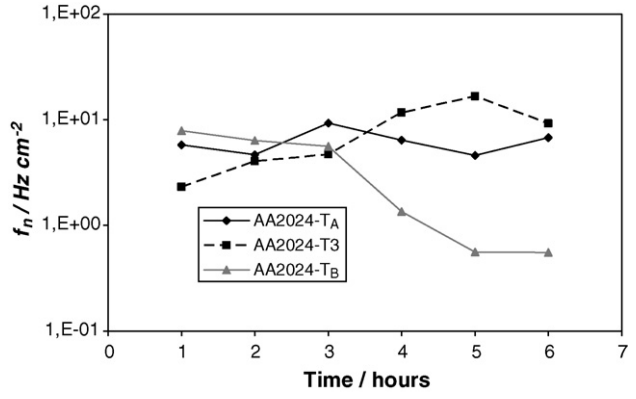

Fig. 18. f_n values of AA2024 samples in NaCl 5.7% and H_2O_2 0.3% solutions at 30 °C, in function of the heat treatment and the immersion time.

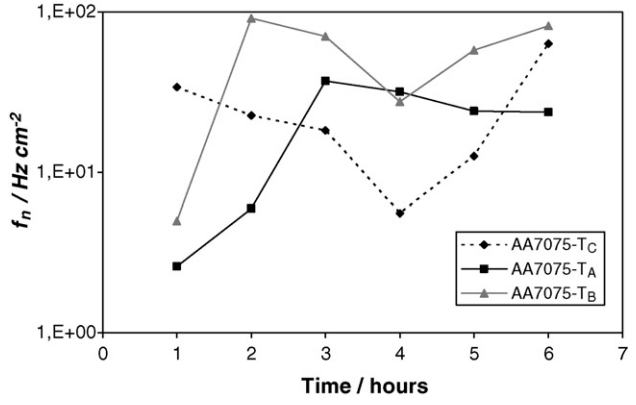

Fig. 20. f_n values of AA7075 samples in NaCl 5.7% and H_2O_2 0.3% solutions at 30 °C, in function of the heat treatment and the immersion time.

degree of IGC is similar in all cases. In fact, due to the special microstructure of the alloy AA7075, the degree of attack never exceeds the degree "A" defined in Table 3.

From the analysis of Figs. 17 and 19, it can be observed that q values in the tests performed with AA7075 samples (q between 3×10^{-6} and 5.7×10^{-4} C) are slightly lower than the values obtained with AA2024 samples (q between 1.9×10^{-5} and 4.8×10^{-4} C). In contrast, it can be appreciated in Figs. 18 and 20 that the f_n values obtained with AA7075 (f_n between 2.6 and 92 Hz cm^{-2}) are slightly higher than those corresponding to AA2024 samples (f_n between 0.5 and 17 Hz cm^{-2}). These data indicate that, in general terms, EN records of AA2024 samples show fewer events with higher charge than the records of AA7075 samples. It can also be observed in these figures that the trend of the values of shot noise parameters is different in the two alloys studied here. Thus, the heat treatment that causes the highest susceptibility to IGC in both alloys, T_B, in AA2024 samples leads to high q and low f_n after the third hour of test, while in AA7075 samples produces the lowest q and the highest f_n values. Therefore, in AA2024 samples, the higher the susceptibility to IGC, the higher the resulting q value and the lower the resulting f_n value. On the contrary, in AA7075 samples, the higher the susceptibility to IGC, the lower the q and the higher the f_n values.

In Figs. 21 and 22, the values of the shot noise parameters obtained in this work and those obtained in [18] for AA2014 samples, have been plotted for purposes of comparison. It can be seen in Fig. 21 that q values of the systems studied here (AA2024 and AA7075 samples) are very high, between 10^{-5} and 10^{-3} C, if they are compared with results reported in [18], where the alloy AA2014 in NaCl solutions led to q values between 10^{-6} and 10^{-5} C. On the other hand, in Fig. 22 it can be appreciated that most f_n values of AA2024 and AA7075 samples fall in the range between 1 and 100 Hz cm^{-2}. It can be commented that

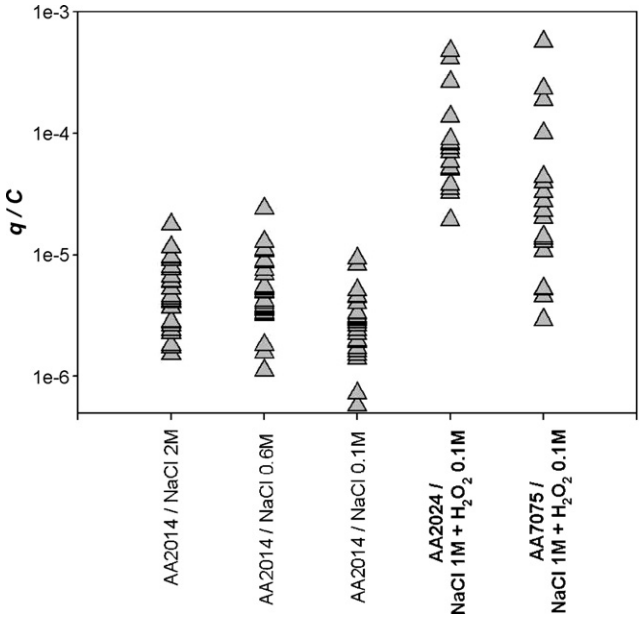

Fig. 21. Comparison between q values for AA2024 and AA7075 obtained in the performed IGC tests and q values reported in the literature [18] for AA2014.

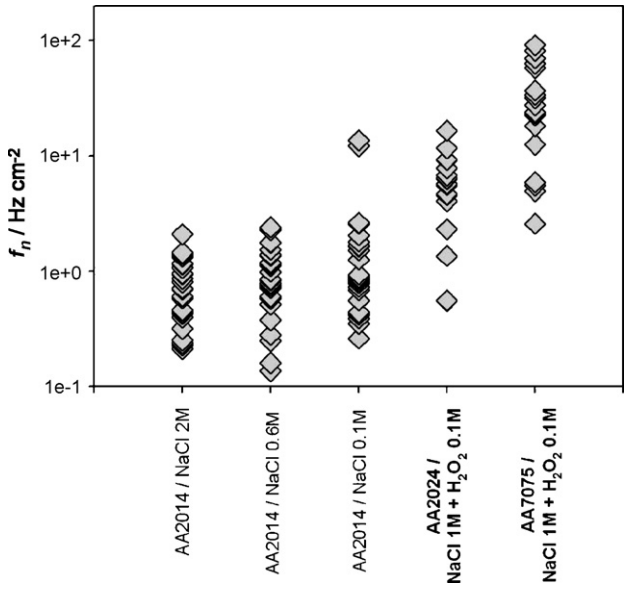

Fig. 22. Comparison between f_n values for AA2024 and AA7075 obtained in the performed IGC tests and f_n values reported in the literature [18] for AA2014.

shot noise is a theory whose assumptions are very strict and quite difficult to be fully satisfied by EN signals. Thus, in the signals studied, EN events are not independent and do not have the same charge and shape [18]. However, these requirements must be assumed to apply the shot noise theory and estimate the q and f_n values. As a consequence, the values of these parameters should be taken into account only for comparative purposes between different systems, since the f_n values are higher than the sampling rate (2.16 Hz). No direct correspondence exists between calculated f_n values (assumed to be independent) and actual number of events (dependent). Therefore, the sampling rate is considered to be adequate, as an adequate anti-aliasing filter was used, not showing the PSDs a plateau at the high frequency range, Figs. 13 and 14. The f_n values of the studied systems are higher than those observed for AA2014 in NaCl solutions, where most f_n values were between 0.1 and 3 Hz cm^{-2} [18]. The differences found between shot noise values of the systems studied here and those studied in [18] are believed to be due to the electrolyte reactivity. Thus, the medium for conducting the IGC tests (NaCl 1 M + H_2O_2 0.1 M) is much more aggressive than the media employed in [18] to promote pitting corrosion (NaCl 0.1, 0.6 and 2 M). As a consequence, higher values of q and f_n are obtained in the IGC tests.

From the analysis of Figs. 17–20, it can be deduced that neither q nor f_n values clearly permit the discrimination between the different heat treatments, that is, the shot noise parameters do not seem to have a high sensitivity to the different degrees of IGC in the samples. However, the systems studied in the present work are characterized by showing both localized corrosion and high activity. The PSD_E and PSD_I spectra were seen to be very unstable in the low frequency range, zone where both q and f_n are calculated, probably due to the high systems activity. In addition, all the hypotheses considered by the shot noise theory may not be satisfied in the real EN records. Thus, the records neither show a clear base line nor have fluctuations of the same ampli-

tude (events of the same charge) [18]. Therefore, it is thought that both the high activity and high localization of the attacks are the reasons why the shot noise parameters of all the systems studied here were quite similar.

4. Conclusions

This paper reports a study of the behaviour against IGC of samples of two aluminium alloys widely employed in the aeronautical industry, AA2024 and AA7075. Samples of these alloys were subjected to different heat treatments, with the object of modifying their susceptibility to IGC. Specifically, two steps of the heat treatment process were changed: the solution heat treatment and the quenching. It has been proved that the heat treatment with a slow quenching step leads to samples with high susceptibility to IGC in both alloys.

In order to determine the susceptibility to IGC of the aluminium alloy samples, normalized tests were carried out; these are based on the immersion of the samples in an aggressive solution in controlled conditions. A metallographic analysis of the samples was performed after the tests to evaluate the amount of IGC suffered by these samples. In order to quantify the corrosion damage produced in these tests, measurements of both the depth of attack and the degree of IGC were carried out.

The experimental setup employed was designed to measure electrochemical noise signals during the normalized IGC tests. These signals were analysed by means of three parameters: noise resistance (R_n) and two shot noise parameters: the characteristic charge (q) and the characteristic frequency (f_n). In the final part of the study, the results of the EN analysis were compared with the results obtained from the metallographic evaluation.

Of the three parameters used to analyse the EN signals, it was determined that R_n provided the best results. In most of the systems studied in this work, the R_n values of IGC tests allow the discrimination between different activities, measured as depths of attacks. Thus, in most cases, it has been proved that the higher the R_n the lower the system activity. Only in some AA7075 samples the correlation between the corrosion activity and the R_n values was found to be poor.

The shot noise parameters, q and f_n, were calculated in order to obtain information related to the degree of IGC suffered by the systems studied. The values of these parameters showed different trends in function of the aluminium alloy tested. Thus, AA2024 samples with high susceptibility to IGC led to relatively high values of q and low values of f_n. Meanwhile, samples of the same alloy with low susceptibility to IGC presented low charge and high frequency. Therefore, in AA2024 samples, it seems that the higher the susceptibility to IGC, the higher the q and the lower the f_n values. In contrast, AA7075 samples showed shot noise parameters with the opposite tendency. Thus, AA7075 samples with high susceptibility to IGC presented relatively low values of q and high values of f_n, while samples with high resistance to IGC presented high charge and low frequency. Consequently, high degrees of IGC in AA7075 samples seem to lead to low q values and high f_n values.

In this paper, systems showing different degrees of susceptibility to IGC were studied, although all of them show both localized corrosion mechanisms and high activities. For this reason, when shot noise parameters were used to analyse the obtained EN signals, it was not possible to establish great differences between the systems studied. These results should not put into question the validity of shot noise parameters as tools of EN analysis. As has been demonstrated in previous studies dealing with these parameters, their employment permits the discrimination of systems showing higher differences, between their corrosion mechanisms and rates, than the systems studied here.

Acknowledgements

Authors would like to thank the institutions who have supported the development of this work: the Ministerio de Educacion y Ciencia (project MAT2001-3477 and the research fellowship F.P.U. AP2001-3830), the Ministerio de Industria (project PETRI PTR1995-0836-OP) and the Junta de Andalucia.

References

[1] http://aluminium.matter.org.uk.
[2] I.J. Polmear, Light Alloys: Metallurgy of the Light Metals, 3rd ed., Elsevier Science, London, 1995.
[3] D.A. Porter, K.E. Easterling, Phase Transformations in Metals and Alloys, 2nd Ed., Chapman & Hall, 1992.
[4] Heat Treatment of Aluminum Alloys. Aerospace Material Specification: AMS-H-6088B, The Engineering Society for Advancing Mobility: Land Sea Air and Space INTERNATIONAL (SAE), 1999, p. 1.
[5] W. Zhang, G.S. Frankel, Electrochim. Acta 48 (2003) 1193.
[6] G. Svenningsen, J.E. Lein, A. Bjorgum, J.H. Nordlien, Y. Yu, K. Nisancioglu, Corros. Sci. 48 (1) (2006) 226.
[7] G. Svenningsen, M.H. Larsen, J. Walsmley, J.H. Nordlien, K. Nisancioglu, Corros. Sci. 48 (6) (2006) 1528.
[8] G. Svenningsen, M.H. Larsen, J.H. Nordlien, K. Nisancioglu, Corros. Sci. 48 (12) (2006) 3969.
[9] H.P. Godard, W.B. Jepson, M.R. Bothwell, R.L. Kane, The Corrosion of Light Metals, John Wiley & Sons Inc., New York, 1967, p. 70.
[10] V. Guillaumin, G. Mankowski, Corrosion 56 (1) (2000) 12.
[11] T.D. Burleigh, E. Ludwiczak, R.A. Petri, Corrosion 51 (1) (1995) 50.
[12] D.A. Eden, Proceedings of the CORROSION/98, Houston, T, U.S.A., NACE (National Association of Corrosion Engineers), Paper no. 386, 1998, p. 1.
[13] S. Turgoose, R.A. Cottis, in: B.C. Syrett (Ed.), Corrosion Testing Made Easy: "Electrochemical Impedance and Noise", NACE International, Houston, U.S.A., 1999, p. 1.
[14] F. Huet, U. Bertocci, C. Gabrielli, M. Keddam, Proceedings of the CORROSION/97 Research Topical Symposia, Part I—Advanced Monitoring and Analytical Techniques, New Orleans, LA, 1998, p. 11.
[15] J.R. Kearns, J.R. Scully, P.R. Roberge, D.L. Reichert, J.L. Dawson (Eds.), Electrochemical Noise Measurement for Corrosion Applications, ASTM STP 1277, West Conshohocken, PA, U.S.A., 1996, p. 1.
[16] R.A. Cottis, Corrosion 57 (3) (2001) 265.
[17] E. Miranda, M. Bethencourt, M.J. Cano, J.M. Sánchez-Amaya, A. Corzo, J. García de Lomas, J. Botana, M.L. Fardeau, B. Ollivier, Corros. Sci. 48 (2006) 2417.
[18] J.M. Sánchez-Amaya, R.A. Cottis, F.J. Botana, Corros. Sci. 47 (2005) 3280.
[19] J.M. Sánchez-Amaya, F.J. Botana, M. Bethencourt, Corrosion 61 (11) (2005) 1050.
[20] A. Aballe, M. Bethencourt, F.J. Botana, M. Marcos, J.M. Sánchez-Amaya, Electrochim. Acta 46 (2001) 2353.
[21] K.-H. Na, S.-I. Pyun, Electrochim. Acta 52 (2007) 4363.
[22] Practice for Evaluating Intergranular Corrosion Resistance of Heat-Treatable Aluminum Alloys by Immersion in Sodium Chloride + Hydrogen

Peroxide Solution ASTM G-110-92, American Society for Testing and Materials, 2003.
[23] I. Arrieta, A. Sagüés, B. Joseph, Proceedings of the CORROSION/2004, New Orleans, LA, NACE, Paper no. 04456, 2004, p. 1.
[24] K. Nachstedt, K.E. Heusler, Electrochim. Acta 33 (3) (1988) 311.
[25] R.A. Cottis, S. Turgoose, Mater. Sci. Forum 192–194 (1995) 663.
[26] J.W. Isaac, K.R. Hebert, J. Electrochem. Soc. 146 (2) (1999) 502.
[27] M. Danielson, Corrosion 53 (10) (1997) 770.
[28] P.C. Pistorius, Corrosion 53 (4) (1997) 273.
[29] I.N. Bastos, F. Huet, R.P. Nogueira, P. Rousseau, J. Electrochem. Soc. 147 (2000) 671.
[30] D.A. Eden, K. Hladky, D.G. John, J.L. Dawson, Proceedings of the Corrosion/86, Houston, T, NACE, Paper no. 274, 1986.
[31] A.N. Rotwell, D.A. Eden, Proceedings of the CORROSION/92, Houston, T, U.S.A., NACE, Paper no. 223, 1992.
[32] R.A. Cottis, M.A.A. Al-Awadhi, H.A. Al-Mazeedi, S. Turgoose, Electrochim. Acta 46 (2001) 3665.
[33] H.A. Al-Mazeedi, R.A. Cottis, Electrochim. Acta 49 (2004) 2787.
[34] A.A. El-Moneim, Corros. Sci. 46 (2004) 2517.
[35] U. Bertocci, F. Huet, Corrosion 51 (2) (1995) 131.
[36] H.A. Al-Mazeedi, R.A. Cottis, S. Turgoose, Eurocorr 2000, Institute of Materials, London, 2000, p. 1.
[37] J.J. de Damborenea, B. Fernández, in: J.R. Kearns, J.R. Scully, P.R. Roberge, D.L. Reichert, J.L. Dawson (Eds.), Paper from the Book: "Electrochemical Noise Measurement for Corrosion Applications", ASTM, West Conshohocken, U.S.A, 1996, p. 398.